Quantifying Land Use/Land Cover Change and Urban Expansion in Dongguan, China, From 1987 to 2020

Peng Dou and Zhen Han

***Abstract*—Dongguan has experienced the most rapid urbanization since the Chinese reform and opening policy. To analyze the urban expansion in this city, in this study, 12 land use/land cover maps were produced using a multiple classifiers system on the Google Earth Engine platform. A long time-series land use dataset from 1987 to 2020, was achieved. The results indicate that, during the past 33 years, the urban area increased by 13.84 times and reached 1483.06 km^2 in 2020, whereas cultivated land and forest continually decreased because of rapid urbanization. By analyzing the changes in urban forms and landscape indexes, Dongguan experienced a diffusion–coalescence–diffusion phase, and its urban expansion can be divided into three stages: The early-age urbanization stage (1987–1996), the rapid urbanization stage (1996–2011), and the intensive urbanization stage (2011–2020). The development of the economic and dual-level administration of Dongguan expanded the urban area surrounding the towns and traffic corridors, and, finally, formed a connected urban area. The urban expansion, just like sparking spots firing the prairie, is special and conforms to a Dongguan urbanization pattern.**

***Index Terms*—Google Earth Engine (GEE), LULC, multiple classifiers system (MCS), remote sensing (RS), urbanization.**

I. Introduction

URBAN constitutes the most concentrated area of human activity, and it is the home of over half of humans. Urbanization refers to the population shift from rural to urban areas, and it is a phenomenon that links many disciplines, including economic development, industrialization, modernization, urban planning, and policy [1]–[3]. Hence, the places that experienced urbanization became the most dramatic land use/land cover (LULC)-changed areas globally [4], [5]. Urbanization is a long-term continuous process that improves socioeconomic development and quality of life [5], [6]. However, it also causes serious problems, such as biodiversity damage, water pollution, urban heat islands, and other environmental problems [7]–[9]. To solve these problems, urbanization studies have become a research hotspot in different fields [1]–[9].

The urbanization pattern is among the most important indicators reflecting a city's economic development and expansion characteristics [10], [11]. The evolution of urban spatial patterns and related social and economic changes play an important role in sustainable development. It helps urban planners and managers to understand the development of residents and economic activities. Many studies have summarized the general urban spatial structure: the concentric ring structure the multiple nuclei structure and the urban realm structure [12]–[14]. However, no structures are well applicable to all cities due to the dynamic change process of urbanization [15]. Camagni *et al.* [16] summed five popular urban growth forms, including infilling, expansion, linear development, sprawl, and large-scale projects. Dietzel considered that the urbanization process occurs in a wave shape change between diffusion and coalescence [17]. Xu *et al.* [18] further developed this hypothesis and verified the diffusion–coalescence phase transition. Liu *et al.* [19] identified the urban as infilling, edge expansion, and outlying for quantifying urban expansion. Dou and Chen [20] studied urban expansion in Shenzhen, China, and illustrated that its urban expansion is a mixture of three different expansion patterns. All these studies indicate that a few cities could be expanded with a single form, and they must be a variant or a mixture of the different growth forms.

LULC change is the most direct expression of urbanization. To better understand this process, a long-term urban LULC dataset is urgently needed. Thanks to the satellite of remote sensing (RS), it provides high spatial and temporal resolution images worldwide; specifically, since the 1970s, the Landsat programme has provided abundant images through Landsat 1–8, thereby making the long time series dynamic monitoring of urban LULC available [20], [21]. Up to now, many LULC datasets, such as the National Land Cover Database and China's Land Use/Cover Dataset, have been produced and can be used to quantify urban expansion [22], [23]. However, these datasets have large time intervals between different years and short time intervals in a time span; thus, Gong released annual maps of global artificial impervious areas between 1985 and 2018 to analyze urban expansion with a higher temporal density [24]. These existing datasets are reliable and effective. However, for some specific areas, it is necessary to extract LULC with higher accuracy using classification methods [20], [25]. Therefore, using Landsat to extract LULC and to study urbanization has become the main approach for most related studies [21]–[26].

Manuscript received November 18, 2021; accepted November 24, 2021. Date of publication December 9, 2021; date of current version December 24, 2021. This work was supported in part by National Natural Science Foundation of China under Grant 42001370, and Grant 42130113, in part by the China Postdoctoral Science Foundation under Grant 2019TQ0233 and Grant 2019M662698, and in part by the Basic Research Innovative Groups of Gansu province, China, under Grant 21JR7RA068. *(Corresponding author: Peng Dou.)*

Peng Dou is with the Key Laboratory of Remote Sensing of Gansu Province, Heihe Remote Sensing Experimental Research Station, Northwest Institute of Eco-Environment and Resources, Chinese Academy of Sciences, Lanzhou 730000, China, and also with the School of Resource and Environmental Sciences, Wuhan University, Wuhan 430079, China (e-mail: dp_imgclassifier@163.com).

Zhen Han is with the QingDao Marine Remote Sensing Information Technology Company, Ltd, QingDao 266000, China (e-mail: hanzhen_hz@126.com).

Digital Object Identifier 10.1109/JSTARS.2021.3133703

Since the reform and opening, China has experienced rapid urbanization [20], [26], [27]–[30]. As one of the three largest Chinese urban agglomerations, the Pearl River Delta region experienced the highest urbanization rate, leading to the emergence of super metropolises, such as Guangzhou, Shenzhen, and Dongguan [20], [26], [28], [30]–[31]. Dongguan is a typical city in these metropolises, which has changed from a small fishery town to a large international metropolitan [30]. Its economic development and urbanization speed are some of the fastest among Chinese cities in history. The development of Dongguan has attracted many scholars to explore its urbanization using RS images. For example, Li and Yeh [31] (1997) analyzed the urban expansion of Dongguan city using three Landsat images acquired in 1988, 1990, and 1993, and the results showed that many of the farmlands in some towns were seized during urbanization. Li *et al.* [32] (2009) proposed that Dongguan city expansion went through a diffusion-polymerization and axial extension-axial filling process using RS images in 1988, 1993, 1997, 2001, 2003, and 2005. Liu *et al.* [19] (2010), using the Landsat images in 1988, 1993, 1997, 2001, and 2006, developed the landscape expansion index for quantifying urban expansion, and the results revealed that urbanization in Dongguan city experienced a diffusion-polymerization phase transition. Feng *et al.* [33] (2014) showed that road network density and weighted nuclear density were highly correlated with new urban land in Dongguan city. These studies utilized limited RS images in the early and middle urban development stages but did not cover the whole process of urban growth up to 2020. This means that the urban growth process was not entirely characterized.

The primary objective of this study was to enhance the understanding of the urbanization pattern and the underlying mechanism in Dongguan based on the time series of urban LULC data from 1987 to 2020 using the Landsat imageries.

The rest of this article is organized as follows. Section II describes the study area and data processing. Section III introduces the methods of classification, postprocessing, urban expansion form and analysis, and other related work. Section IV exhibits the results and Section V presents the discussion. Finally, Section VI concludes this article.

II. Study Area and Materials

A. Study Area

Dongguan is located on the east coast of the Pearl River Bay (113°30′–114°15′E, 22°39′–23°08′N) between Guangzhou City (capital city of Guangdong Province, China) and Shenzhen City (Fig. 1) [34]. The south and southeast of Dongguan are mountainous regions. Mountains and hills are mainly distributed in this area, with elevation increasing from north to southeast. The Dongjiang River, the most important river in this city, flows through the region in the north and northeast. The Dongjiang alluvial delta plain lies in its northwest area, with many low-lying water networks. The north and middle regions are the nursery area with a low altitude. The southwest area is at the brink of the Pearl River estuary alluvial plain [35]. Before 1985, Dongguan was a typical Chinese agricultural county. In 1985, the Pearl River Delta Area Economic Development Zone was established by the Chinese State Council in Dongguan County, which was then renamed Dongguan City at the county level. Later in 1988, it was promoted to the city level. Dongguan City has a dual-level administration structure, including four districts (i.e., Dongguan, Nancheng, Dongcheng, and Wangjiang) and 28 towns (Table I).

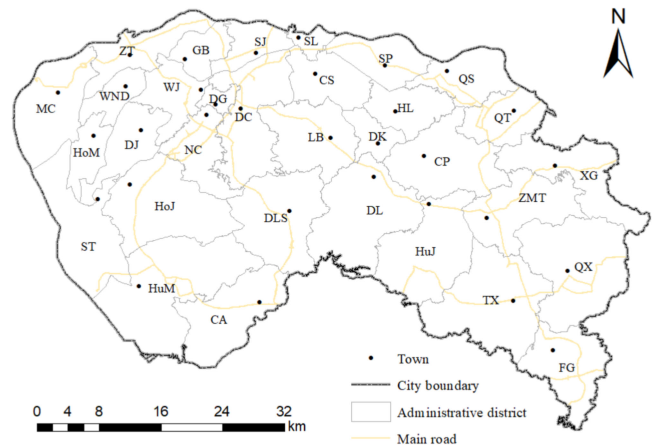

Fig. 1. Schematic map of Dongguan City.

TABLE I
Districts and Towns in Dongguan

Name	Abbreviation	Name	Abbreviation
Dongguan	DG	Daojiao	DJ
Nancheng	NC	Houjie	HoJ
Dongcheng	DC	Huangjiang	HuJ
Wangjiang	WJ	Dalingshan	DLS
Qiaotou	QT	Changping	CP
Hongmei	HoM	Qingxi	QX
Changan	CA	Fenggang	FG
Machong	MC	Tangxia	TX
Shatian	ST	Gaobu	GB
Humen	HuM	Shijie	SJ
Wangniudun	WND	Zhongtang	ZT
Dongkeng	DK	Dalang	DL
Liaobu	LB	Zhangmutou	ZMT
Xiegang	XG	Qishi	QS
Hengli	HL	Chashan	CS
Shilong	SL	Shipai	SP

B. Data Description

1) Landsat Imagery: Since Dongguan was promoted to city status in 1985, this city experienced dramatic urbanization highlighted by rapid growth. To estimate the land use/cover change, Landsat 5 TM and Landsat 8 OLI time series images with WRS path 122 and row 44 were employed in this study. Images from 1987 to 2020, with intervals of three years, were selected on the Google Earth Engine (GEE) platform. To reduce the effect of clouds on classification, most images with cloud cover of more than 10% were filtered, and the remaining images were transformed to surface reflectance data using the GEE function "ee.Algorithms.Landsat.calibratedRadiance" [36]. All images

TABLE II
INFORMATION OF RS IMAGE COLLECTIONS AND TRAINING SAMPLES

Year	Satellite & sensor	Number of RS images	Number of training samples						
			Forest	Grassland	Cultivated land	Built-up area	Bare land	Water body	Total
1987	Landsat TM	4	815	712	856	840	856	800	4897
1990	Landsat TM	5	806	826	888	890	799	783	4892
1993	Landsat TM	3	820	804	852	859	811	842	4888
1996	Landsat TM	3	811	800	820	866	821	838	4956
1999	Landsat TM	6	791	809	800	803	802	793	4798
2002	Landsat TM	4	821	820	856	835	822	838	4992
2005	Landsat TM	3	798	802	813	806	809	804	4832
2008	Landsat TM	4	801	775	799	803	806	793	4777
2011	Landsat TM	3	806	823	821	835	803	862	4950
2014	Landsat OLI	6	810	818	830	824	816	807	4905
2017	Landsat OLI	5	833	834	833	830	839	831	5000
2020	Landsat OLI	4	813	822	808	821	828	832	4924

were geometrically registered with the geographic coordinate system of the World Geodetic System 1984 (WGS_1984), and the pixel size was set to 30 m. Overall, 12 years were selected to generate stable LULC maps with their corresponding multiple temporal RS images. The number of RS images in each collection can be find in Table II.

2) Land-Use Types, Interpretation Sign,s and Samples: The study area was divided into six LULC types: forest, grassland, cultivated land, built-up area, bare land, and water body. High-resolution RS images of Google Earth were used as reference data to identify the different LULC types from Landsat images. Google Earth provided high-resolution images only after 2002; thus, we used interpretation signs describing the features of LULC types on the Landsat image to assist in the sample selection of images acquired before 2002 [20]. As we aimed to produce a stable LULC map, all sampling regions had no obvious changes in LULC within at least one year, and all pixels in the sample polygons were pure. All samples were used for training, and their information is shown in Table II.

III. METHODS

A. LULC Classification

GEE is a cloud platform dedicated to geographic data processing and analysis. It provides massive RS data and excellent image-processing algorithms, and it enables researchers to perform large-scale and long-term analyzes with minimal cost and equipment [37]. In the field of LULC extraction, GEE has been considered the most effective tool, and it has been used to produce many LULC products [23], [24], [37]. In this article, we used GEE as the platform and designed a multiple classifiers system (MCS) for LULC classification. The scheme of the classification is as follows. First, Landsat images were collected and filtered to generate an image collection. Second, for each image, sample polygons were used to extract pixels to train a classifier called a base classifier. As LULC types in the sampling regions were stable within one year, all classifiers would not be affected by incorrectly labeled samples. Third, using the base classifiers, an MCS was structured. Taking the images in the collection as input, different LULC maps were produced. Finally, the most common value at each pixel across the stack of all LULC maps was calculated, and a more accurate map that could reflect a stable LULC status was produced.

GEE has provided several excellent supervized classification algorithms, such as support vector machines, decision tree, naive Bayes, random forest (RF), and gradient tree boost [37], [38]. In this study, we used the most commonly used RF to train base classifiers in the MCS. The number of trees in the RF was set to 100. Using the MCS on the GEE platform, we obtained 12 LULC maps in different years from 1987 to 2020.

B. Data Postprocessing

After classification, using an eight-connected filter, raster polygons smaller than two pixels were removed and replaced with the pixel value of the largest neighbor polygon. To identify the potential wrongly classified pixels, we used a method that overlapped the previous LULC map layer with the latter to obtain the changed LULC regions [20]. If the LULC changes in this region were illogical, the LULC on both map layers should be checked and correlated. In this article, the illogical transformations include built-up area to cultivated land, built-up area to forest, built-up area to grassland, and built-up area to water body. We treat them as illogical transformation, because in most LULC changes, this transformation might be rare or preposterous. After the potential wrongly classified regions were identified, we repeatedly modified the LULCs to ensure that the data had the highest accuracy as possible.

C. Urban Expansion and LULC Analysis Methods

1) Correlation Analysis: Urbanization is a complicated process that accompanies economic and social development. This article analyzes the correlation between the urbanization rate and related factors during development using Statistical Product and Service Solutions software [39]. As urban expansion is closely related to economy and population, gross domestic product (GDP), population, and total investment in fixed assets (TIIFA) were used in the analysis. Economic development attracts more people and more investment, thus promoting urban expansion [20], [26], [40].

TABLE III
DESCRIPTION OF URBAN FORMS

Urban form	Description
EX	A standard form of expansion where land use is a development directly adjacent to the existing land use.
IN	New developments are set in areas that were previously unused or being redeveloped to new uses.
SP	A standard form of suburban development taking advantage of scattered lots.
LD	The expansion that is shaped by an existing corridor of circulation.

TABLE IV
DESCRIPTION OF LANDSCAPE INDEXES

Landscape index	Comments
Area-weighted mean fractal dimension index (FRAC_AM)	Reflects shape complexity of landscape types; if the value is close to 1, the shape of landscape is simple, otherwise the shape is complex. Range: 1≤FRAC_AM≤2.
Number of patches (NP)	Reflects the degree of landscape fragmentation; the greater the NP value, the higher the fragmentation degree. Range: NP≥1.
Largest path index (LPI)	Quantifies the percentage of total landscape area comprised by the largest patch. As such, it is a simple measure of dominance. Range: 0<LPI≤1.
Edge Density (ED)	Edge density reports edge length on a per unit area basis that facilitates comparison among landscapes of varying size. Range: ED ⩾ 0.

2) Urban Expansion Forms: The literature has grouped urban expansion forms into different types. For example, Angel *et al.* [42] classified urban expansion into main urban core, secondary urban core, urban fringe, ribbon development, and scatter development [41]. Camagni *et al.* [16] divided urban expansion into five general types: Infilling, extension, linear development, sprawl, and large-scale projects. However, for Dongguan City, which was developed from discretely distributed towns and villages, using the same standard makes it difficult to analyze urban expansion throughout the research range. Referencing preresearch, this article analyzed urban expansion, first, by dividing urban land into urban core and nonurban core and, second, by dividing urban land into infilling (IN), extension (EX), linear development (LD), and sprawl (SP).

Based on the dynamic development view, we chose some urban land patches as the foundation area of the following year. We calculated the average area of the urban land paths in 12 years and screened out the urban land patch, which had an area larger than 0.1 km^2, as the core urban area, which could reflect the skeleton characteristics of urban growth. The paths smaller than 0.1 km^2 were set as the nonurban core, which consisted of some scattered residential areas. The definitions of IN, EX, LD, and SP are listed in Table III [16], [43].

3) Urban Landscape Metrics: Landscape metrics have been extensively applied in previous research to study urban development characteristics [44]. This article chose the number of patches (NP), edge density (ED), landscape shape index (LSI), and area-weighted mean fractal dimension index (FRAC_AM) to calculate the metrics using Fragstats 4.2. The landscape indices used in this study are described in Table IV [44].

IV. RESULTS

A. LULC Estimation

To improve classification accuracy, the automatically estimated LULC results were postprocessed through manual interpretation. Using the LULC drive from the RS classification, 1000 samples in each class were randomly selected and checked using high-resolution RS images from Google Earth as the reference data. The average of the overall accuracy reached 89.88%, and the confusion matrix is illustrated in Fig. 2. The dominant land use types, such as built-up area, cultivated land, and forests, have

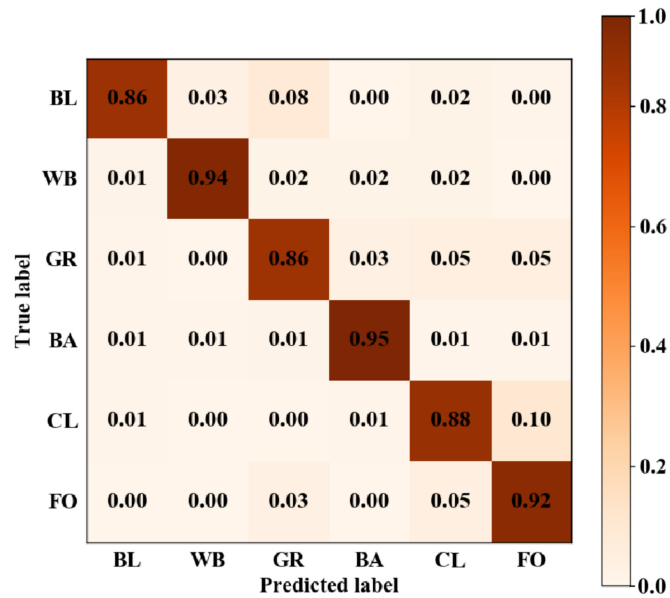

Fig. 2. Confusion matrix of the classification results BL: Bare land; WB: Water body; GR: Grassland; BA: Built-up area; CL: Cultivated land; FO: Forest.

accuracy of over 88%, and the built-up area which represents the urban land has high accuracy of 95.00%. The result is reasonable and could be used for analyzing the urbanization pattern of Dongguan.

Fig. 3 illustrates the LULC change in Dongguan. The built-up area had the most dramatic changes among all the LULC types. Cultivated land forests decreased year by year. From 1132.18 km^2 in 1987 to 228.84 km^2 in 2020, cultivated land decreased by 1103.36 km^2 at an average rate of 2.95% per year. Forest land decreased at an average annual reduction rate of 1.33%, less than that for cultivated land. The water body area was stable, and bare land showed an unstable fluctuating trend due to land development. Before a large increase in built-up areas, bare land would increase to a certain extent; this increase is related to the process of LULC conversion to built-up areas.

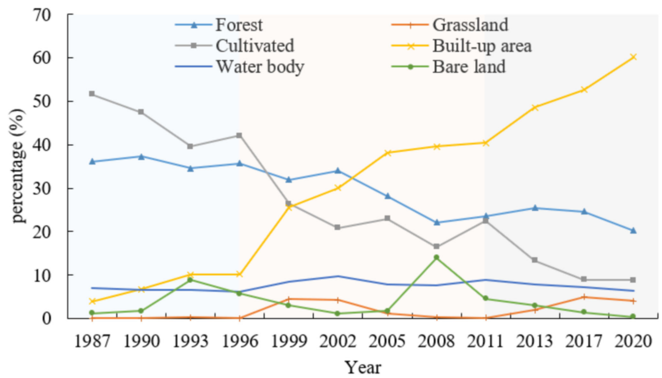

Fig. 3. LULC changes in Dongguan from 1987 to 2020.

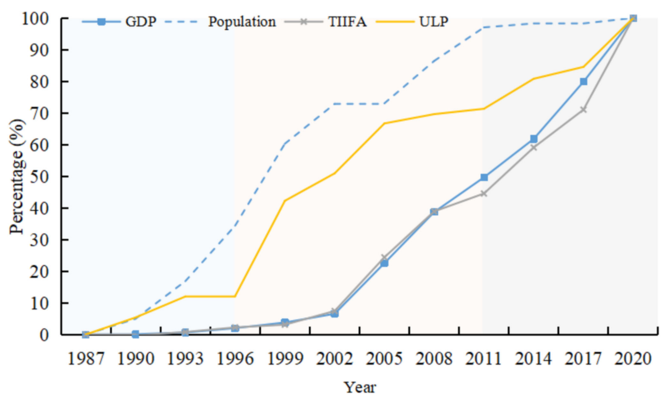

Fig. 4. Temporal changes in ULP and the economy in Dongguan City from 1987 to 2020.

TABLE V
AREA AND PERCENTAGES OF DIFFERENT URBAN LAND FORMS

Year	Urban land (km^2)	Percentage (%)		
		ULP	UCP	NUCP
1987	107.13	3.98	7.97	92.03
1990	181.05	6.73	9.50	90.50
1993	272.04	10.12	18.52	81.48
1996	273.75	10.18	30.35	69.65
1999	688.12	25.59	38.66	61.34
2002	807.67	30.03	43.56	56.44
2005	1024.53	38.10	51.09	48.91
2008	1064.86	39.60	58.59	41.41
2011	1088.39	40.47	62.38	37.62
2014	1218.75	45.32	75.94	24.06
2017	1270.31	47.24	81.09	18.91
2020	1483.06	55.15	92.28	7.72

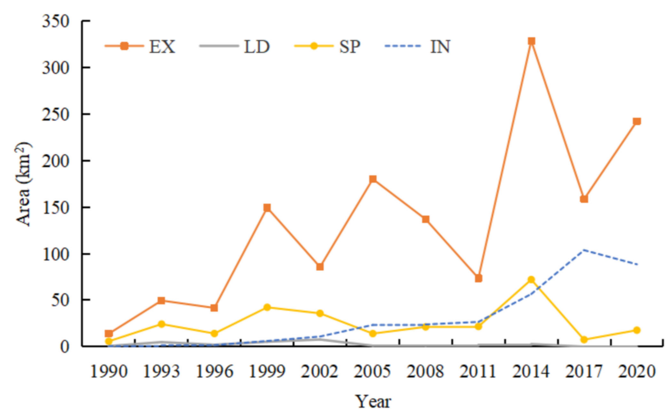

Fig. 5. Area changes of EX, LD, SP, and IN.

Grassland constituted a small percentage of the whole area, and during the study period, its area percentage remained below 6%.

B. Change in Urban Land and Economic Indexes

Table II lists area of urban land in different years. For a better description, it also shows urban land percentage to the whole study area (short as ULP), urban core percentage to the whole urban land (short as UCP), and nonurban core to the whole urban land (short as NUCP). In 1987, the urban land area was only about 107.13 km^2, accounting for 3.98% of the entire city area. After a continuous increasing trend over 33 years, urban land increased 13.84 times and reached 1483.06 km^2 in 2020, and the highest increasing speed occurred from 1996 to 1999. The increased area accounted for 15.41% of the entire city. After 2005, the built-up area became the largest area among the six LULC types.

This study collected data on the ULP, GDP, population, and TIIFA. For comparison, Fig. 4 shows the ratio of each year's data to the largest data of each factor. The ULP and the population had a clear increasing trend from 1987 to 2020. The GDP and TIIFA increased slowly before 2002, and their ratios were 6.54% and 7.42%, respectively. After 2002, the economy started to take off, and both the GDP and TIIFA exhibited a dramatic, continuous increasing trend.

The ULP represents the expansion state of the urban area. A correlation analysis showed that the GDP, population, and TIIFA had a very significant positive correlation with the ULP, and that the correlation coefficients were 0.886, 0.97, and 0.891, respectively. These features indicate that the population and the economy are important reasons for the rapid expansion of this city.

C. Temporal Changes in Urban Forms

Table V shows that the UCP in 1987 was 7.97% and that 92.03% of the urban area was a nonurban core area. After 1987, the UCP increased, and in 2005, it reached 51.09%, surpassing the NUCP as the main urban land type. In 2020, the UCP reached 92.28%, indicating that most urban land became the main urban area.

Fig. 5 illustrates the area of urban expansion forms of EX, LD, SP, and IN in each year. Clearly, EX was the main urban expansion form from 1990 to 2020. From 1990 to 1999, SP was the second main urban expansion form, and it showed an increasing trend. The area of SP decreased after 1999, and it was the third main urban expansion form in 2005. The IN form showed an increasing trend, and after 2005, it became the second urban expansion form instead of SP; after 2011, it showed a dramatic growth trend. This could be due to the fact that, with the continuous shortage of usable land, vacant land within the city gradually became occupied, and new developments were

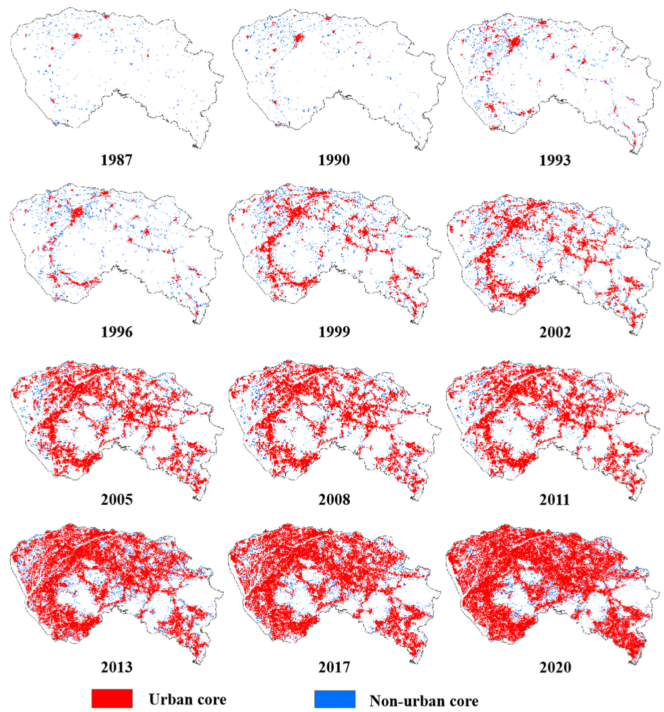

Fig. 6. Spatial distribution of core urban and noncore urban areas.

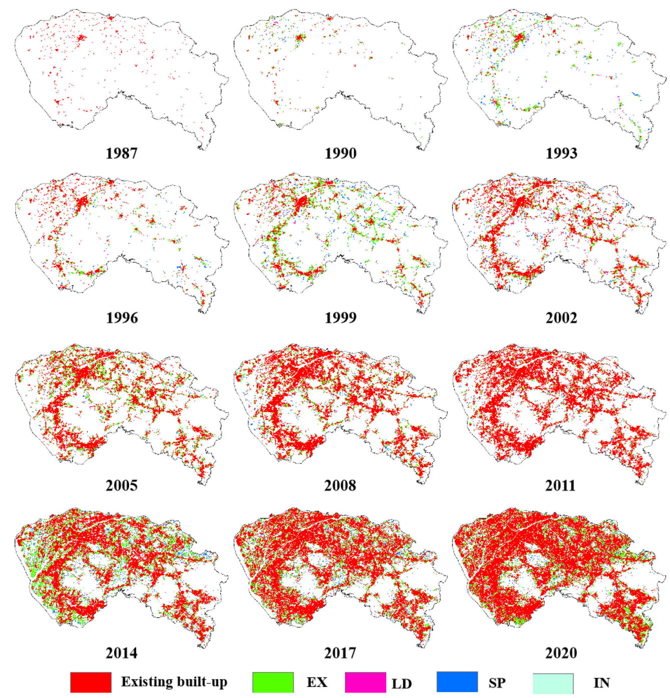

Fig. 7. Spatial distribution of EBU, EX, LD, SP, and IN.

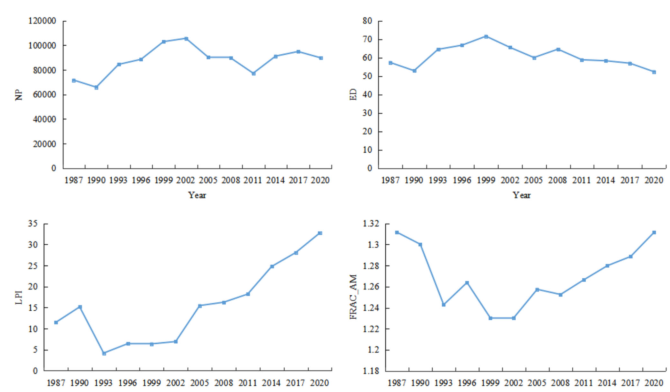

Fig. 8. Changes in the different landscape metrics in Dongguan.

set in areas that were previously unused or redeveloped to new uses.

D. Urban Spatial Expansion Forms

The urban core showed different spatial changes. As shown in Fig. 6, the urban core experienced a dramatic expansion. In 1987, the urban core was very small, mainly distributed around the DG district, and point-shaped distributed in SL, DJ, DL, and TX. The areas were then expanded along with other towns growing in the urban cores from 1987 to 1999. During this time, the nonurban core was scatter distributed. In 2002, the main core urban areas were connected and formed a multiple-core urban pattern. After 2005, the urban core in the entire city began to connect into an integrated core in the midwest region, changing from 523.43 km^2 in 2005 to the highest at 1368.56 km^2 in 2020. The UCP reached its highest at 92.28% in 2020.

Fig. 7 shows the distribution of EX, LD, and IN in different years. From 1987 to 1999, most of the core urban areas of the city grew with an EX form, and the noncore urban areas were mainly an SP form. The LD and IN accounted for small proportions. After 2002, the core urban area became a single entity, the scattered residential areas gradually merged with the main urban area, and the EX became the main urban form of urban expansion. Since 2011, the city has experienced a large-scale expansion. In less than 10 years, the urban area increased from 1088.39 km^2 in 2011 to 1483.06 km^2 in 2020, with an increase of 36.29%.

Combining the urban core, EX, LD, and IN forms together, urban land in Dongguan had an obvious spatial characteristic developed from the sporadic dot distribution of urban land, and it finally formed a multigroup coordinated development pattern surrounding the DG district, including the large western arc strip development zone, the central group integrated development zone and the southeast group development zone. The urbanization process was based in many towns, followed by the simultaneous expansion around the towns and traffic corridors, finally forming an urban land connectivity distribution in a large area. This dynamic spatio–temporal urbanization pattern was similar to sparkling spots in a prairie, and the development was similar to a seafire, with the towns looking like sparkling spots. We called this spatial urban expansion the Dongguan pattern.

E. Landscape Metrics

This paper calculated four landscape metrics. As illustrated in Fig. 8, LSI showed a continuously decreasing trend in 1987, a minimum value in 2013, only 31.80% in 1987, and a slight rebound in 2015. NP increased in 1987, reached a peak in 1996, had a decreasing fluctuation and reached the minimum value in 2011. ED showed an increasing trend, had a lower value in 2003 and 2005 than in 2001 and reached the highest value in 2015.

The NP and ED had different change trends. They showed a synchronous increasing trend from 1987 to 1996. After 1996, in contrast to the decreasing trend in NP, ED had an increasing trend. From 1996 to 1999, NP almost had the fastest decreasing trend. The change trend of NP and ED recovered the same trend after 2001. From 2001 to 2003, NP had the same decreasing rate as that from 1996 to 1999, but the change rate of ED was different from that in 1999. NP and ED both had decreasing trends. After 2011, the NP and ED had the same obvious increasing trend.

V. Discussion

A. Characteristics of Urbanization At Different Stages

Over the past three decades, Dongguan has experienced rapid urbanization. Fig. 3 illustrates the growth process of the urban area. According to the increasing curve, the process of urbanization can be divided into three stages: Early-age urbanization stage (1987–1996), rapid urbanization stage (1996–2011), and intensive urbanization stage (2011–2020).

The results of the landscape metrics showed that NP and ED had increasing trends from 1987 to 1996, indicating that with the growth of towns and the continuous emergence of scattered residential areas, the landscape of the entire region began to fragment. Clearly, during this period, the urban growth of the city was dominated by the SP form. This feature led to a decreasing proportion of large urban patches, resulting in the LPI decreasing from its initial high value. Note that the FRAC_AM also decreased, probably due to the core urban areas being gradually connected in this stage (Fig. 6), thus simplifying the shape of the urban patches.

From 1996 to 2011, as the expansion of the city was gradually being dominated by the EX form, NP and ED decreased, and the fragmentation of the urban landscape lessened. As the core urban area was connected as a whole, the PLI gradually increased because of urban expansion. The FRAC_AM also increased, indicating that the geometric shapes of the urban landscape were becoming more and more complex.

After 2011, the NP exhibited a slight increase, probably due to the large-scale development in this stage (Figs. 3 and 6), which increased the degree of landscape fragmentation. As the urban areas became more connected and the geometric shapes of the urban landscape became more complex, both LPI and FRAC_AM increased.

The diffusion–coalescence transition in urban expansion has been considered a dynamic spatial–temporal process, as demonstrated in many cities [17], [18], [20]. The changes in the urban forms of Dongguan also experienced diffusion and coalescence. A diffusion process occurred from 1987 to 1996. The main characteristics of this process are the increase in NP and the continuous appearance of SP. From 1996 to 2011, SP and NP showed obvious decreasing trends, and the scatter developments continuously merged with the larger core urban areas (Fig. 6), resulting in a continuous increase in LPI. This indicates a coalescence process during this period. This process continued after 2011, but some diffusion processes still occurred with increasing SP during this period, causing a slight increase in NP in 2014.

B. Urban Expansion is Affected by the Economy

The rapid urbanization of Dongguan was closely related to the development of its economic activities. At the start of the urbanization phase, Dongguan was just a county administrator, mainly based on agriculture. Through the Chinese reform and opening-up policy and the establishment of the Pearl River Delta special economic zone, Dongguan adopted the “three processing and one compensation” model [45]. The economic and correlation auxiliary facilities underwent great development, and the increasing investment, foreign investment, and road constructions gave more foundation conditions for economic development. Moreover, in this stage, the “three processing and one compensation” industry, which was mainly labor-intensive light industry, attracted more people to Dongguan. This explains why the economic growth ratio was lower than that of the population and the ULP during the diffusion process from 1987 to 1996.

To benefit from economic development and to accommodate different social needs, more buildings were constructed to accommodate more industries and markets, while residential areas expanded to house an increasing number of people. This led to a continuous increase in urban land. In turn, the increase in urban land gave a good foundation condition and environment to economic activities, attracting more people and investment. In this way, the urban land area and economic and social development during the entire period exhibited a coupling development relationship, promoted each other, and turned urban development from a diffusion process into a coalescence process.

After 2011, Dongguan’s population growth slowed and maintained a stable state, while economic development continued to increase. Investment in real estate increased from 373.3×10^8 yuan in 2011 to 965.02×10^8 yuan in 2020 by 158.51%, indicating the acceleration of real estate development. With the rapid development of real estate and the lack and high cost of internal development in Dongguan, real estate mainly focused on the construction of point neighborhood units in the suburbs and the development of correlation ancillary facilities. All of these were responsible for the diffusion trend of urban land from 2020.

C. Pattern of Urbanization in Dongguan

Urbanization featuring a diffusion–coalescence phase transition is a dynamic change process. As shown in Fig. 6, the urbanization pattern is similar to sparkling spots that set fire to a prairie. It is a special development model, unlike the ribbon expansion model, in which urban growth expands from several centers [46]. The urban spots in the Dongguan pattern are not only simple business and recreation centers but also administrator centers. Almost all towns developed independently at the same time. It is different from the radiated model, in which urban areas extend from urban centers to surrounding areas in all directions in a series of concentric circles [46]. It is also different from the satellite model, in which the urban satellite has a larger scale than the town area and fewer points than the sparkling spots [47]. The urban land spots in the Dongguan pattern started as the residential distribution spots around the administrator center, finally coming to end at the economic, urban, and administrator centers. With the economic and policy changes, urban land around large numbers of spots underwent rapid development and formed a large area with an integrated urban land distribution.

Whether there are similar urbanization processes in other places has yet to be determined. The special pattern of urbanization in Dongguan may be related to the city's administration structure. In Dongguan, the dual-level administration structure is operated by the city government as the first administration body and the town government as the second administration body. This administration structure is different from that of most Chinese cities that employ a three-level administration structure, which includes the city government, the county government, and the town government.

The 32 towns of the city had an outstanding effect on Dongguan's urbanization. As Dongguan was promoted to the city level in 1988, the Dongguan government implemented material processing, sample processing, contract assembly, and compensation trade policies. Economic policy promotes the development of industries in each town. No matter the towns' industrial development agglomeration being based on the local or international market, the same industries concentrated in one region, and the leading industry supported regional economic development. Moreover, one town had typical industries and specialized collaborations and promoted rural urbanization to expand in Dongguan [48].

The development of towns served as a foundation for the urbanization of the Dongguan pattern. Based on the dual-level administration structure and the different natural and social conditions, the towns had different economic development speeds, and some towns were intended to be the cores, similar to sparkling spots. With economic development, the sparkling spots connected with the traffic network, making the urban core areas exhibit a concentrated trend and forming a multigroup coordinated development pattern. With the development of towns and the increase in connections, the urban planning of Dongguan underwent small adjustments, and urban land was divided into the northwest special development zone, southwest coast new urban, middle region high-quality urban centre, northeast industrial integration development demonstration zone, and southeast modern industrial development agglomeration area [35]. This is another confirmation of the development process of the Dongguan pattern.

VI. Conclusion

In this study, 12 temporal LULC maps were produced using an MCS on the GEE platform and achieved a high-accuracy urban land-use dataset of Dongguan for urban expansion analysis. From 1987 to 2020, Dongguan experienced rapid urbanization, and its urban land changed from a small land type to the largest land type. Urbanization is a process of diffusion–coalescence–diffusion phase transition and has unique development.

Economic development and the increasing population provided a driving force for the urbanization process in Dongguan. Different from other cities, the dual-level administration structure in Dongguan produced a unique spatial urbanization pattern. Under the dual-level administration structure and special economic policies, the towns developed independently in the initial stage until they finally formed coordinated development. This dynamic spatio–temporal urbanization pattern was similar to sparkling spots in a prairie, and development was similar to a seafire, with the towns looking like sparkling spots. This spatial urbanization pattern was called the Dongguan pattern. Unlike other urban growth hypotheses, the Dongguan pattern is a complex result of economic and political changes based on a dual-level administrator structure. The Dongguan pattern is also a combination of urban forms and the urban growth phase transition. As this urbanization pattern has gathered different opinions and to determine whether this pattern has occurred in other cities, further study is needed on urbanization in the world.

Acknowledgment

The authors would like to thank the editors and anonymous reviewers for their valuable suggestions.

References

[1] X. Liang, X. Liu, G. Chen, J. Leng, Y. Wen, and G. Chen, "Coupling fuzzy clustering and cellular automata based on local maxima of development potential to model urban emergence and expansion in economic development zones," *Int. J. Geographical Inf. Sci.*, vol. 34, no. 10, pp. 1930–1952, Mar. 2020.

[2] Q. Zhang and S. Su, "Determinants of urban expansion and their relative importance: A comparative analysis of 30 major metropolitans in China," *Habitat Int.*, vol. 58, pp. 89–107, 2016.

[3] S. Li, C. Zhou, and S. Wang, "Does modernization affect carbon dioxide emissions? A panel data analysis," *Sci. Total Environ.*, vol. 663, pp. 426–435, May 2019.

[4] J. Hu and Y. Zhang, "Seasonal change of land-use/land-cover (LULC) detection using MODIS data in rapid urbanization regions: A case study of the Pearl River delta region (China)," *IEEE J. Sel. Topics Appl. Earth Observ. Remote Sens.*, vol. 6, no. 4, pp. 1913–1920, Aug. 2013.

[5] S. S. Bhatti, N. K. Tripathi, M. Nagai, and V. Nitivattananon, "Spatial interrelationships of quality of life with land use/land cover, demography and urbanization," *Soc. Indicators Res.*, vol. 132, no. 3, pp. 1193–1216, Apr. 2016.

[6] M. Hofmann, S. Münster, and J. R. Noennig, "A theoretical framework for the evaluation of massive digital participation systems in urban planning," *J. Geovisualization Spatial Anal.*, vol. 4, no. 1, p. 3, Dec. 2019.

[7] H. Zhao, X. Duan, B. Stewart, B. You, and X. Jiang, "Spatial correlations between urbanization and river water pollution in the heavily polluted area of Taihu Lake Basin, China," *J. Geographical Sciences*, vol. 23, no. 4, pp. 735–752, Jun. 2013.

[8] X. Zhou and H. Chen, "Impact of urbanization-related land use land cover changes and urban morphology changes on the urban heat island phenomenon," *Sci. Total Environ.*, vol. 635, pp. 1467–1476, Sep. 2018.

[9] C. A. Iserhard, L. Duarte, N. Seraphim, and A. V. L. Freitas, "How urbanization affects multiple dimensions of biodiversity in tropical butterfly assemblages," *Biodiversity Conservation*, vol. 28, no. 3, pp. 621–638, Dec. 2018.

[10] B. Bhatta, S. Saraswati, and D. Bandyopadhyay, "Urban sprawl measurement from remote sensing data," *Appl. Geography*, vol. 30, no. 4, pp. 731–740, Dec. 2010.

[11] L. Jiao, "Urban land density function: A new method to characterize urban expansion," *Landscape Urban Planning*, vol. 139, pp. 26–39, Jul. 2015.

[12] W. Kuang, W. Chi, D. Lu, and Y. Dou, "A comparative analysis of megacity expansions in China and the U.S.: Patterns, rates and driving forces," *Landscape Urban Planning*, vol. 132, pp. 121–135, Dec. 2014.

[13] C. D. Harris and E. L. Ullman, "The nature of cities," *Ann. Amer. Acad. Political Social Sci.*, vol. 242, no. 1, pp. 7–17, 1945.

[14] T. A. Hartshorn, *Interpreting the City: An Urban Geography*. Hoboken, NJ, USA: Wiley, 1992.

[15] E. H. Wilson, J. D. Hurd, D. L. Civco, M. P. Prisloe, and C. Arnold, "Development of a geospatial model to quantify, describe and map urban growth," *Remote Sens. Environ.*, vol. 86, no. 3, pp. 275–285, 2003.

[16] R. Camagni, M. C. Gibelli, and P. Rigamonti, "Urban mobility and urban form: The social and environmental costs of different patterns of urban expansion," *Ecological Econ.*, vol. 40, no. 2, pp. 199–216, Feb. 2002.

[17] C. Dietzel, M. Herold, J. J. Hemphill, and K. C. Clarke, "Spatio-temporal dynamics in California's Central Valley: Empirical links to urban theory," *Int. J. Geo-Inf. Sci.*, vol. 19, no. 2, pp. 175–195, 2005.

[18] C. Xu, M. Liu, C. Zhang, S. An, W. Yu, and J. M. Chen, "The spatiotemporal dynamics of rapid urban growth in the Nanjing metropolitan region of China," *Landscape Ecology*, vol. 22, no. 6, pp. 925–937, 2007.

[19] X. Liu, X. Li, Y. Chen, Z. Tan, S. Li, and B. Ai, "A new landscape index for quantifying urban expansion using multi-temporal remotely sensed data," *Landscape Ecology*, vol. 25, no. 5, pp. 671–682, 2010.

[20] P. Dou and Y. Chen, "Dynamic monitoring of land-use/land-cover change and urban expansion in Shenzhen using landsat imagery from 1988 to 2015," *Int. J. Remote Sens.*, vol. 38, no. 19, pp. 5388–5407, Jun. 2017.

[21] P. Fu and Q. Weng, "A time series analysis of urbanization induced land use and land cover change and its impact on land surface temperature with landsat imagery," *Remote Sens. Environ.*, vol. 175, pp. 205–214, Mar. 2016.

[22] M. L. Smith, W. Zhou, M. Cadenasso, M. Grove, and L. E. Band, "Evaluation of the national land cover database for hydrologic applications in urban and Suburban Baltimore, Maryland," *J. Amer. Water Resour. Assoc.*, vol. 46, no. 2, pp. 429–442, Jan. 2010.

[23] W. Kuang, S. Zhang, X. Li, and D. Lu, "A 30-meter resolution dataset of China's urban impervious surface area and green space fractions, 2000–2018," *Earth System Sci. Data*, vol. 13, pp. 63–82, 2021.

[24] P. Gong *et al.*, "Annual maps of global artificial impervious area (GAIA) between 1985 and 2018," *Remote Sens. Environ.*, vol. 236, Jan. 2020, Art. no. 111510.

[25] X. Zhao *et al.*, "Joint classification of hyperspectral and LiDAR data using hierarchical random walk and deep CNN architecture," *IEEE Trans. Geosci. Remote Sens.*, vol. 58, no. 10. pp. 7355–7370, Oct. 2020.

[26] Y. He, P. Dou, H. Yan, L. Zhang, and S. Yang, "Quantifying the main urban area expansion of Guangzhou using landsat imagery," *Int. J. Remote Sens.*, vol. 39, no. 21, pp. 7693–7717, Jul. 2018.

[27] J. Chen, J. Gao, and W. Chen, "Urban land expansion and the transitional mechanisms in Nanjing, China," *Habitat Int.*, vol. 53, pp. 274–283, 2016.

[28] J. Ou, X. Liu, X. Li, Y. Chen, and J. Li, "Quantifying spatiotemporal dynamics of urban growth modes in metropolitan cities of China: Beijing, Shanghai, Tianjin, and Guangzhou," *J. Urban Planning Develop.*, vol. 143, no. 1, 2017, Art. no. 04016023.

[29] W. Wu, S. Zhao, C. Zhu, and J. Jiang, "A comparative study of urban expansion in Beijing, Tianjin and Shijiazhuang over the past three decades," *Landscape Urban Planning*, vol. 134, pp. 93–106, 2015.

[30] Dongguan Bureau of Statistics, Dongguan, China. [Online]. Available: http://tjj.dg.gov.cn/tjnj/index.html

[31] X. Li and A. G.-O. Yeh, "Application of remote sensing for monitoring and analysis of urban expansion a case study of Dongguan," *Geographical Res.*, vol. 16, no. 4, pp. 56–62, 1997.

[32] S. Li, X. Li, X. Liu, and Y. Chen, "A model of axial urban spatio-temporal Dynamics—-A case study in Dongguan, in Guangdong Province," *Urban Stud.*, no. 9, pp. 17, 2009.

[33] Z. X. Feng, Y. X. Chen, Q. L. Qian, and S. S. Wang, " Relationship between the structure of urban traffic network and urban spatial expansion: A case study of Dongguan City," *J. Geo-Inf. Sci.*, vol. 16, pp. 79–86, 2014.

[34] B. S. Dongguan, *Dongguan Statistical Yearbook (2014)*. Beijing, China: Chinese Statistics Press, 2015.

[35] X. Li and A. G. O. Yeh, "Analyzing spatial restructuring of land use patterns in a fast growing region using remote sensing and GIS," *Landscape Urban Planning*, vol. 69, no. 4, pp. 335–354, 2004.

[36] Google Earth Engine, [Online]. Available: https://developers.google.com/earth-engine/apidocs/ee-algorithms-landsat-calibratedradiance

[37] Y. Wang, Z. Li, C. Zeng, G.-S. Xia, and H. Shen, "An urban water extraction method combining deep learning and Google Earth Engine," *IEEE J. Sel. Topics Appl. Earth Observ. Remote Sens.*, vol. 13, pp. 769–782, 2020.

[38] A. Tassi and M. Vizzari, "Object-Oriented LULC classification in Google Earth Engine combining SNIC, GLCM, and machine learning algorithms," *Remote Sens.*, vol. 12, no. 22, Nov. 2020, Art. no. 3776.

[39] SPSS (Statistical Product and Service Solutions), 2015. [Online]. Available: https://moam.info/spss-statistical-product-and-service-solutions_59d06fd81723ddd486a2c2ca.html

[40] C. J. Liao, J. F. Huang, L. Sheng, and H. Y. You, "Grey correlation analysis between urban built-up area expansion and social economic factors: A case study of Hangzhou, China," *Appl. Mechanics Materials*, vol. 209–211, pp. 1615–1619, Oct. 2012.

[41] L. N. Kantakumar, S. Kumar, and K. Schneider, "Spatiotemporal urban expansion in Pune metropolis, India using remote sensing," *Habitat Int.*, vol. 51, pp. 11–22, 2016.

[42] S. Angel, J. Parent, and D. Civco, "Urban sprawl metrics: An analysis of global urban expansion using GIS," in *Proc. Amer. Soc. Photogrammetry Remote Sens. - ASPRS Annu. Conf. 2007: Identif. Geosp. Sol.*, vol. 1, 2007, pp. 22–33.

[43] The Geography of Transport Systems, [Online]. Available: https://transportgeography.org/contents/chapter8/urban-land-use-transportation/urban-expansion/

[44] UMass Landscape Ecology Lab., Amherst, MA, USA, "FRAGSTATS: Spatial pattern analysis program for categorical maps," 2015, Accessed January 23 2015. [Online]. Available: http://www.umass.edu/landeco/research/fragstats/down loads/fragstats_downloads.html. UNCED. 1992. Agenda 21

[45] A. G. O. Yeh and J. Xu, *China's Pan-Pearl River Delta: Regional Cooperation and Development*. A. G. O. Yeh and J. Xu, Eds., Hong Kong: Hong Kong Univ, 2011, pp. 1–243.

[46] H. Zhao, L. Ma, L. Wang, and J. Li, "Examining urban expansion using multi-temporal landsat imagery: A case study of montreal census metropolitan area," in *Proc. IEEE Int. Geosci. Remote Sens. Symp.*, 2016, pp. 2869–2872.

[47] B. Romano, F. Zullo, L. Fiorini, S. Ciabò, and A. Marucci, "Sprinkling: An approach to describe urbanization dynamics in Italy," *Sustainability (Switzerland)*, vol. 9, no. 1, 2017, Art. no. 97.

[48] K. C. Seto and M. Fragkias, "Quantifying spatiotemporal patterns of urban land-use change in four cities of China with time series landscape metrics," *Landscape Ecology.*, vol. 20, no. 7, pp. 871–888, 2005.

Peng Dou received the M.S. degree in cartography and geography information system from Lanzhoujiaotong University, Lanzhou, China, in 2014, the Ph.D. degree in cartography and geography information system from Sun Yat-sen University, Guangzhou, China, in 2018.

He is currently a Postdoctoral Researcher with the School of Resource and Environmental Sciences, Wuhan University, Wuhan, China. His research interests include remote sensing image classification, urbanization dynamic detection, and image processing.

Zhen Han received the B.S. degree from Shandong Normal University, Jinan, China, in 2011, the M.S. degree in cartography and geography information system from Lanzhoujiaotong University, Lanzhou, China, in 2014.

He is currently the CEO of QingDao Marine Remote Sensing Information Technology Company, Ltd. His research interests include remote sensing technology and geographic information system.